
ALICE: An Interpretable Neural Architecture for Generalization in Substitution Ciphers

Jeff Shen* & Lindsay M. Smith*

Princeton University

Princeton, NJ 08540, USA

{shenjeff, lindsay.smith}@princeton.edu

Abstract

We present cryptogram solving as an ideal testbed for studying neural network generalization in combinatorially complex domains. In this task, models must decrypt text encoded with substitution ciphers, choosing from $26!$ possible mappings without explicit access to the cipher. We develop ALICE (an Architecture for Learning Interpretable Cryptogram dEcipherment): a simple encoder-only Transformer that sets a new state-of-the-art for both accuracy and speed on this decryption problem. Surprisingly, ALICE generalizes to unseen ciphers after training on only ~ 1500 unique ciphers, a minute fraction (3.7×10^{-24}) of the possible cipher space. To enhance interpretability, we introduce a novel bijective decoding head that explicitly models permutations via the Gumbel-Sinkhorn method, enabling direct extraction of learned cipher mappings. Through early exit analysis, we reveal how ALICE progressively refines its predictions in a way that appears to mirror common human strategies for this task: early layers employ frequency-based heuristics, middle layers form word structures, and final layers correct individual characters. Our architectural innovations and analysis methods extend beyond cryptograms to any domain with bijective mappings and combinatorial structure, offering new insights into neural network generalization and interpretability.

1 Introduction

A cryptogram is a type of puzzle in which a piece of text is encrypted using a substitution cipher, and the user’s task is to recover the original plaintext by inferring the cipher used for the encryption. Users typically solve cryptograms based on prior knowledge about language letter frequency distributions and common words. Originally developed for real encryption purposes, they are now popular in newspapers and puzzle books for entertainment purposes due to their simplicity (i.e., lack of real security). This simplicity, however, provides a unique testbed for testing and understanding generalization and reasoning in neural networks.

1.1 Cryptogram task

In a one-to-one monoalphabetic substitution cipher, each letter in a fixed alphabet is mapped to a unique substitute character; this cipher represents a bijective mapping over the alphabet. While other ciphers exist (e.g., Vigenère cipher, Playfair cipher), we focus here on one-to-one monoalphabetic substitution ciphers, as the problem space is combinatorially complex while remaining structurally simple to interpret. We hereafter mean one-to-one monoalphabetic substitution cipher when we say “cipher”, unless otherwise specified.

More formally, let Σ be a finite alphabet of size V representing allowable characters (e.g., 26 for the English alphabet). Then S_V is the symmetric group on Σ containing all bijections from Σ to itself. Importantly, the cardinality of S_V is $|S_V| = V!$. Each cipher mapping $f : \Sigma \rightarrow \Sigma$ is a permutation

*Equal contribution.

for Σ , with $f \in S_V$. Let $\mathbf{x} = (x_1, x_2, \dots, x_L) \in \Sigma^L$ be a plaintext sequence of characters (i.e., in English) and $\mathbf{c} = (c_1, c_2, \dots, c_L) \in \Sigma^L$, with $c_i = f(x_i), i \in \{1, \dots, L\}$ be the corresponding ciphertext sequence.

The goal is to develop a model that is trained on example pairs of (\mathbf{c}, \mathbf{x}) , but is never given access to the underlying cipher f . At inference time, the model is tasked with decrypting some ciphertext \mathbf{c} that has been encrypted under an unseen cipher f . That is, the model needs to implicitly infer the inverse cipher mapping f^{-1} and perform $\hat{\mathbf{x}} = f^{-1}(\mathbf{c})$.

This task is combinatorially complex and requires reasoning over a space with $V!$ possible ciphers. Because of the enormous number of possible f , a model that simply memorizes training examples will fail when applied to the decryption of unseen ciphers. Instead, a model that performs well must learn a general algorithm for decryption that will work under any cipher.

1.2 Related work

Cryptogram decryption is a long-studied problem, traditionally tackled through letter- and word-frequency analysis. These approaches typically require human domain knowledge, such as empirical frequency tables or dictionaries, to guide plaintext guesses (see Appendix A for a broader discussion). Neural approaches to substitution ciphers have only recently emerged, starting in 2018 and remaining relatively limited in scope. Gomez et al. [7] applied a discrete GAN to Caesar and Vigenère ciphers without relying on prior frequency statistics or key information. Kambhatla et al. [11] used an LSTM-based character language model with beam search (widths up to 100,000) to evaluate candidate plaintexts. Aldarrab and May [2] introduced a multilingual encoder–decoder Transformer that first remaps ciphertext into a frequency-based representation before autoregressively decoding character by character. More recently, Kambhatla et al. [12] proposed a recurrence encoding scheme with a decoder-only Transformer, extending the task to homophonic ciphers where a single plaintext character may map to multiple ciphertext symbols.

Despite these advances, existing neural methods generally lack interpretability and fail to enforce the bijective constraints fundamental to standard substitution ciphers. Large language models (LLMs) might seem like a natural alternative, but as we show in Appendix H, they often hallucinate and do not respect bijectivity, limiting their effectiveness for cryptogram decipherment.

1.3 Main contributions

We introduce ALICE, a simple encoder-only Transformer that achieves state-of-the-art accuracy and speed in cryptogram solving while serving as a testbed for studying neural generalization. Our contributions are threefold:

Architecture: We develop a novel end-to-end differentiable decoding head that explicitly enforces bijectivity. This architectural innovation is applicable to any domain with bijective mappings (e.g., matching problems, permutation learning) and provides a principled alternative to post-hoc constraint satisfaction or regularization.

Interpretability: ALICE enables direct extraction of learned permutations, eliminating the need for unreliable attention map analysis. Our early exit analysis reveals interpretable decryption strategies that mirror human problem-solving approaches, providing a new perspective on how neural networks reason under structural constraints.

Generalization: We use ALICE to analyze neural network generalization in combinatorially complex domains, showing that robust performance emerges after exposure to only 3.7×10^{-24} of the total task space. This has implications for few-shot learning in structured reasoning tasks.

We release all model and training code publicly at <https://github.com/al-jshen/alice>.

2 Model architecture

ALICE (an Architecture for Learning Interpretable Cryptogram dEcipherments) is a family of encoder-only Transformers [30] designed for cryptogram solving. The backbone follows a LLaMA-style architecture [29] with full quadratic attention, pre-normalization via RMSNorm [32], SwiGLU activations [27], and Rotary Position Embeddings [28]. Panel (a) of Figure 1 illustrates the core architecture shared across all ALICE variants.

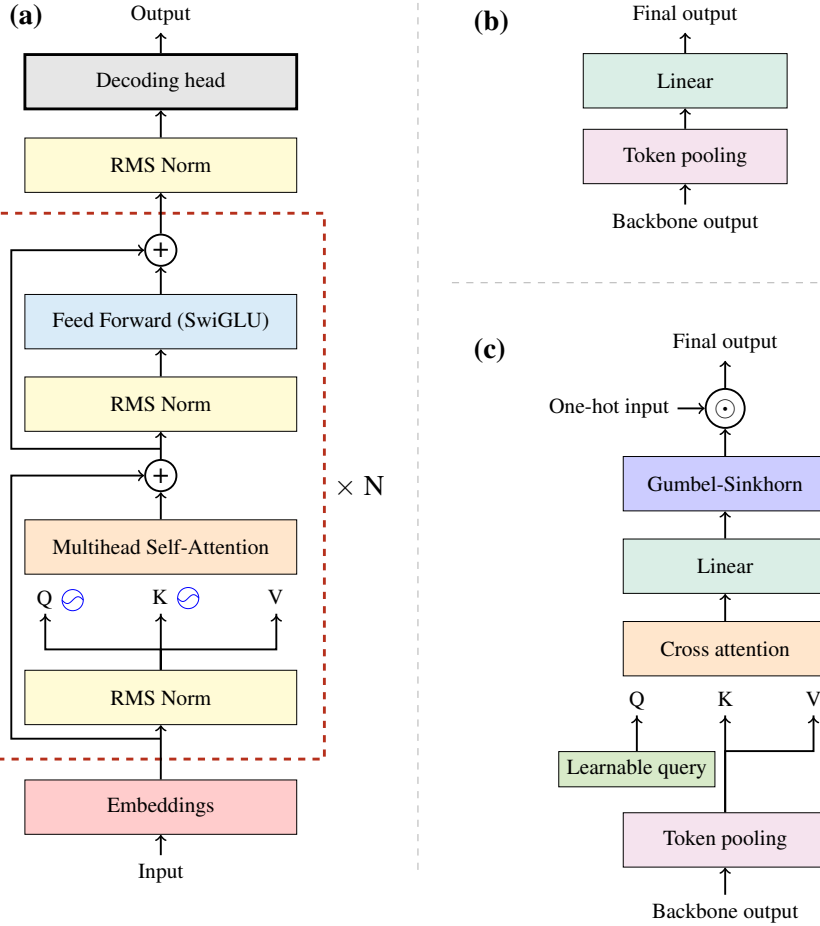


Figure 1: Overview of model architecture. **(a)** Main architecture and description of backbone. The \otimes indicates Rotary Position Embedding [28]. The architectural details of the decoding head are shown on the right two panels. **(b)** Standard decoding head. “Backbone output” indicates the input to the decoding head; this is the representation produced by the encoder model after the final RMSNorm layer. **(c)** Bijective decoding head. “One-hot input” indicates the one-hot encoded version of the original ciphertext input. The \odot indicates a matrix multiplication operator. See Equation 5 for details on the Gumbel-Sinkhorn operation.

We study two models within this framework: ALICE-BASE, which uses a standard linear classification head to map hidden states to symbol predictions. ALICE-BIJECTIVE, which replaces the classification head with a novel end-to-end differentiable bijective decoding head, which we detail in Section 2.1.

Symbol-wise token pooling strategy In the cryptogram setup, each input letter is deterministically mapped to a single output letter. However, an “out-of-the box” standard neural network will not obey this constraint; the same input character appearing in different positions may produce different (i.e., inconsistent) outputs due to varying contextual embeddings. To address this problem, we implement a symbol-wise token pooling strategy. Prior to decoding from the final linear layer to output letters, we average all the embeddings for each unique symbol in the input (e.g., all instance of “A”) and return a single pooled embedding for that symbol. This ensures that repeated symbols are always mapped consistently.

2.1 Bijective decoding

Because we focus on one-to-one cipher mappings in this paper, we design a decoding module that allows ALICE to explicitly learn a bijective cipher mapping f^{-1} ; we dub this variant ALICE-BIJECTIVE. This reduces hallucination and increases interpretability. To our knowledge, ALICE-

BIJECTIVE is the first model explicitly designed with enforced bijectivity between input and output alphabets for solving cryptograms. While models without this bijective decoding module can implicitly learn a mapping f^{-1} , there are typically no constraints on its bijectivity, leading to the possibility of structurally invalid outputs (i.e., two ciphertext letters map to the same plaintext letter), and making it challenging to extract the learned mapping for interpretation.

ALICE-BASE will sometimes predict a mapping that maps two different letters to the same letter:

```
Plaintext:  THE SEA HAS TESTIFIED THAT AFRICA AND EUROPE HAVE KISSED.
Ciphertext: JAE CEH AHC JECJISIEK JAHJ HSOIWH HQK EMOZUE AHDE YICCEK.
Predicted:  THE SEA HAS TESTIFIED THAT AFOICA AND EXOUSE HAVE KISSED.
```

In this example, ALICE-BASE predicts that both the cipher letters ‘C’ and ‘U’ map to the plaintext letter ‘S’ due to a lack of bijective enforcement. We know, however, that under the cryptogram puzzle constraints, this should be impossible.

To mitigate this behavior, we add a new component to ALICE. Architecturally, we add a cross-attention layer with a learnable query after the main transformer blocks to reduce the sequence length of the internal representation to the vocabulary size. We then apply a linear layer, as in the standard architecture, to reduce the model dimension to the vocabulary size. At training time, we then apply Sinkhorn normalization via iterative column- and row-wise normalization to turn this square matrix into a doubly stochastic matrix [14]:

$$S^0(X) = \exp(X) \tag{1}$$

$$S^l(X) = \mathcal{T}_c(\mathcal{T}_r(S^{l-1}(X))) \tag{2}$$

$$S(X) = \lim_{l \rightarrow \infty} S^l(X), \tag{3}$$

where \mathcal{T}_c and \mathcal{T}_r are column and row normalization (i.e., we divide each column value by the sum of its column and each row value by the sum of its row). From this doubly stochastic matrix, we would like to create a corresponding permutation matrix \mathcal{P}^* , typically framed as a linear assignment problem

$$\mathcal{P}^* = M(X) = \arg \max_{P \in P_N} \langle X, P \rangle_F, \tag{4}$$

where P_N is the set of all permutation matrices and $\langle \cdot, \cdot \rangle_F$ is the Frobenius norm. However, as M is not differentiable, we instead draw permutation matrices \mathcal{P} from the Gumbel-Sinkhorn distribution [18]

$$\mathcal{P} \sim S\left(\frac{X + \epsilon}{\tau}\right), \text{ with } \epsilon \sim \text{Gumbel} \tag{5}$$

which is a continuous relaxation of M that is fully differentiable. From this (soft) permutation matrix we can obtain soft decodings of the ciphertext by applying a matrix multiplication with the one-hot encoded inputs. Note that at inference time, we obtain a hard permutation matrix \mathcal{P}^* using $M(X)$, as we do not need the output to be differentiable.

Panels (b) and (c) of Figure 1 show the differences between the ALICE-BASE decoding head and the ALICE-BIJECTIVE decoding head, respectively. ALICE-BASE only needs to learn the action of a mapping $f^{-1}(\cdot)$, and does not need to explicitly model the mapping itself. Thus, to recover the mapping for analysis, one must resort to strategies such as analysis of attention maps, which requires human intervention and can be time consuming as well as unreliable [9, 25]. ALICE-BIJECTIVE explicitly predict a latent permutation matrix, and so extraction/inspection of the learned mappings can be done directly.

3 Numerical experiments

Dataset The main dataset we use is QUOTES500K [6], which consists of 500K English language quotes. We perform basic cleaning, and unless otherwise specified, we keep sequences of lengths 15-300. We also compile a multilingual dataset by taking a small subset of the OSCAR corpus [23] for the following languages: English, French, German, Italian, Latin, Portuguese, and Spanish. For each language, we replace all accented characters with their unaccented counterpart (following

Ciphertext length	<32	32 – 64	64 – 128	128 – 256	>256
ALICE-BASE	6.67 ^{+23.15} _{-6.67}	0.00 ^{+5.56} _{-0.00}	0.00 ^{+0.87} _{-0.00}	0.00 ^{+0.00} _{-0.00}	0.00 ^{+0.00} _{-0.00}
ALICE-DYNAMIC	6.45 ^{+22.69} _{-6.45}	0.00 ^{+5.56} _{-0.00}	0.00 ^{+0.90} _{-0.00}	0.00 ^{+0.00} _{-0.00}	0.00 ^{+0.00} _{-0.00}
ALICE-BIJECTIVE	15.38 ^{+27.47} _{-12.12}	2.17 ^{+8.94} _{-2.17}	0.00 ^{+1.96} _{-0.00}	0.00 ^{+0.00} _{-0.00}	0.00 ^{+0.00} _{-0.00}

Table 1: Median per-character error rate (SER) across different test cipher lengths (lower is better). We compare the standard model (ALICE-BASE), a variant with dynamic embeddings (ALICE-DYNAMIC), and one with bijective decoding (ALICE-BIJECTIVE). Errorbars show the 16–84th percentile range across sequences within each length bin. Ciphertext length includes spaces and punctuation.

Aldarrab and May [2]) and perform similar cleaning as the QUOTES500K dataset. Further details on the dataset construction can be found in Appendix B.

For both the QUOTES500K and our multilingual datasets, we take 97.5% of the sequences as training sequences and the remaining 2.5% as unseen testing sequences. Training examples are encrypted on-the-fly by applying a random substitution cipher to the plaintext, leaving spaces and punctuation unchanged.

Performance evaluation Based on previous work [2, 11, 12, 20], we use the symbol error rate (SER) as our metric for evaluating the performance of our models; this is calculated as the fraction of incorrect symbols in the output of the model (the deciphered text) as compared to the plaintext. We include the encrypted characters, spaces, and punctuation in the SER. We report all SER values as percentages in this text.

3.1 Ablations

To compare different design choices for ALICE, we perform two architecture ablations. The performance of all model variants is shown in Table 1. All models are roughly equal in terms of parameter count, and they are all trained for 100K steps with the same optimizer and hyperparameters and dataset. Further details about training are provided in Appendix C.

Dynamic embeddings Typically, embeddings are vector representations of tokens (letters). When trained on vast amounts of data, the meaning of tokens are learned, so that semantic information is encoded in the embeddings. In the case of cryptograms, while the available input letters stay fixed, the *meaning* of a particular letter changes with the cipher. For example, “A” in ciphertext could either represent “E” or “S” in plaintext, depending on the cipher. This, as pointed out by Aldarrab and May [2], violates the typical assumptions of embeddings. Thus, we want a way to allow for flexibility in the meaning of input tokens.

We experiment with *dynamic embeddings*: we create a hypernetwork to predict the token embeddings based on the input. We dub this variant ALICE-DYNAMIC and provide further architectural details in Appendix D. We hypothesize that this will allow for more flexibility than static embeddings (i.e., shared across all inputs/ciphers), which force “A” to have the same semantic embedding regardless of the cipher it is encoded with. In contrast, dynamic embeddings will allow the meaning of “A” to change with the context.

We find in Table 1 that ALICE-DYNAMIC does not improve performance. Surprisingly, ALICE-BASE performs just as well for all ciphertext lengths, despite the meaning of tokens changing with each example. This is in spite of the fact that ciphertext letters that the model sees have no semantic meaning, as they can correspond to different plaintext letters with each example, whereas ALICE-DYNAMIC can change the semantic meaning of the ciphertext letters given the context. In Figure 6 we use early exit analysis (see also Section 5) and find that while dynamic embeddings improve the immediate guess after the embedding layers, the later transformer blocks of the base architecture allow it to quickly achieve performance parity with the dynamic architecture.

Bijective decoding We use ALICE-BIJECTIVE as described in Section 2, which enforces the structure of the cryptograms task and improves interpretability. We use constant $\tau = 1$ and $\ell = 5$ Sinkhorn normalization iterations (see Equation 3) throughout training.

While performance remains strong—achieving perfect decryption for ciphertexts longer than 64 characters—ALICE-BIJECTIVE lags slightly behind ALICE-BASE, particularly for short (<32) and moderately short (32–64) sequences. We attribute this partly to unoptimized hyperparameters τ and ℓ , which strongly affect stability and accuracy. For instance, lower τ values bring the Gumbel-Sinkhorn distribution closer to $M(X)$ but increase gradient variance. Improved training strategies, such as annealing τ [10, 17], may close the gap with ALICE-BASE.

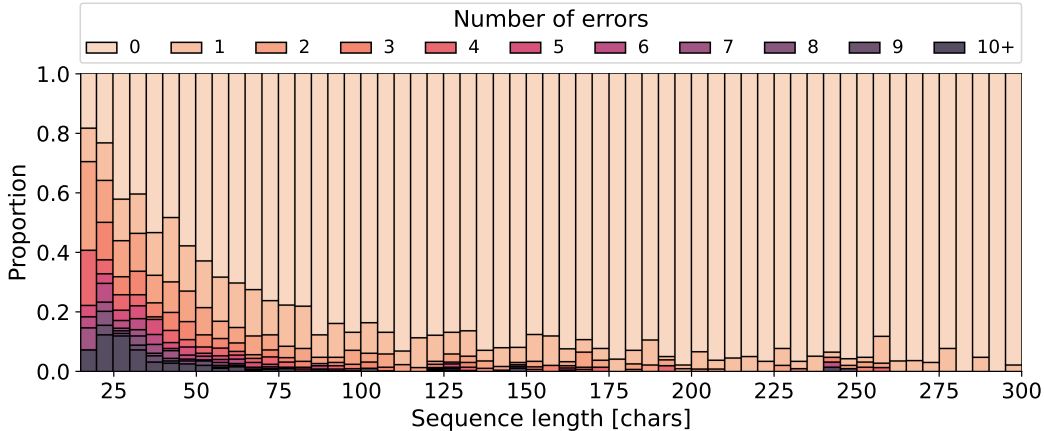


Figure 2: Distributions of number of errors made across various test ciphertext lengths for ALICE-BASE. The sequence length axis has a bin width of 5. Lighter colours indicate fewer errors.

3.2 Model performance

The difficulty of decrypting a cryptogram depends strongly on ciphertext length. Figure 2 shows model error distributions across binned lengths. For very short sequences (<30 characters), the ALICE-BASE often makes 5+ errors—consistent with the unicity distance of English under substitution ciphers [26], which implies such ciphertexts cannot be uniquely decrypted. Beyond this threshold, performance improves rapidly: by ~75 characters, over 90% of sequences contain at most one error, plateauing at ~150 characters where the model is error-free ~95% of the time. Residual errors at long lengths appear due to dataset noise (e.g., typos, improper word breaks).

Table 2 compares ALICE to prior neural deciphering methods. On short sequences (<128 chars), ALICE-BASE achieves a new state of the art, reducing error rates by 84.6% relative to Aldarrab and May [2]. Notably, it outperforms specialized frequency- and recurrence-based models despite using no handcrafted encoding, and even ALICE-BIJECTIVE—less accurate but more interpretable—beats all prior baselines. With error rates of 1–2%, a cipher of length 50 typically contains just a single mistake, still easily interpretable by humans.

Finally, ALICE is not only more accurate but also orders of magnitude faster than the previously fastest algorithm [12] (see Appendix G).

Table 2: Character-level error rate (SER) for various models on short and long sequences. Lower is better.

Ciphertext length →	<128	>128
Beam + 6-gram [20]	22.00%	0.00%
Beam + NLM [11]	10.89%	0.00%
Beam + NLM + Freq. [11]	11.32%	0.00%
Seq2Seq + Freq. [2]	7.68%	0.00%
Causal LM + Freq. [12]	10.56%	0.00%
Causal LM + Recurrence [12]	11.30%	0.02%
ALICE-BASE (this work)	1.18%	0.08%
ALICE-BIJECTIVE (this work)	2.32%	0.14%

Table 3: Performance on decryption of historical Borg cipher with multilingual models. Lower is better.

Model	Error rate (↓)
Seq2Seq [2]	5.47%
Causal LM [12]	4.10%
ALICE-BASE (this work)	2.80%

3.2.1 Multilingual decryption

We train ALICE-BASE on the multilingual dataset described above. During both training and inference time, the information about the language of the text is not provided to the model. As such, ALICE now needs to perform the additional task of identifying the correct underlying plaintext language in order to properly decode the ciphertext. To compare with Kambhatla et al. [12], we evaluate this model on a length-256 cipher from page 0011v of the historical Borg cipher,² a 17th century book handwritten in encrypted Latin text, first automatically decrypted by Aldarrab [1]. We report the performance of ALICE as compared to previous work in Table 3 with two caveats. Firstly, we follow Kambhatla et al. [12] and compare against the performance of Aldarrab and May [2], but we note that Aldarrab and May [2] decrypt a slightly different input, corresponding to page 0002r of the Borg cipher. Secondly, the error rate of our model varies slightly depending on the transcription of the cipher. That is, a different ciphertext tokenization mapping results in slightly different outputs from the model. We thus report the mean of 100 runs, although performance on individual runs varies from 0.00% to 6.25%.

4 Model generalization

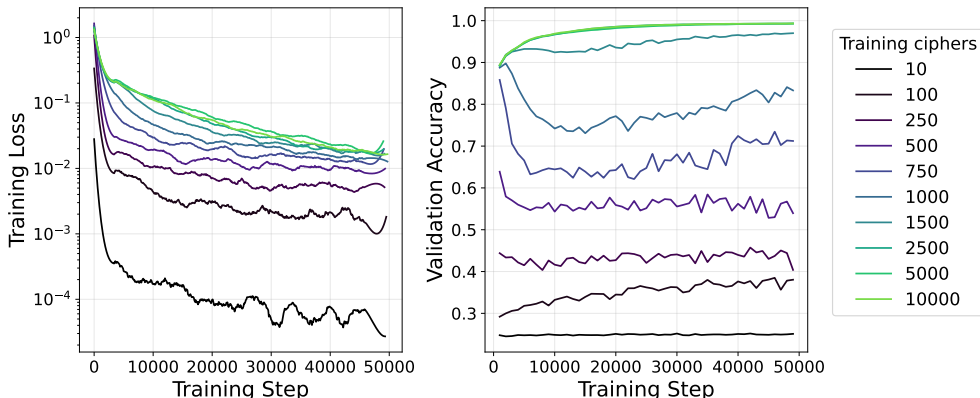


Figure 3: Generalization experiments. **Left:** Training loss vs. step with a Savitzky-Golay filter applied for smoothing. **Right:** Validation accuracy vs. training step. ALICE-BASE trained on fewer ciphers achieves lower training error but does not generalize to unseen ciphers. The number of training ciphers needed to generalize to near perfect accuracy on unseen ciphers is very low (~ 1500).

We investigate how the number of distinct ciphers (“tasks”) seen during training affects generalization ciphers. We note here that this task space contains $26!$ possible ciphers, making memorization infeasible; thus, strong performance on unseen ciphers indicates true generalization. If the model has learned a general “cryptogram-solving solution,” then accuracy on held-out ciphers should remain high.

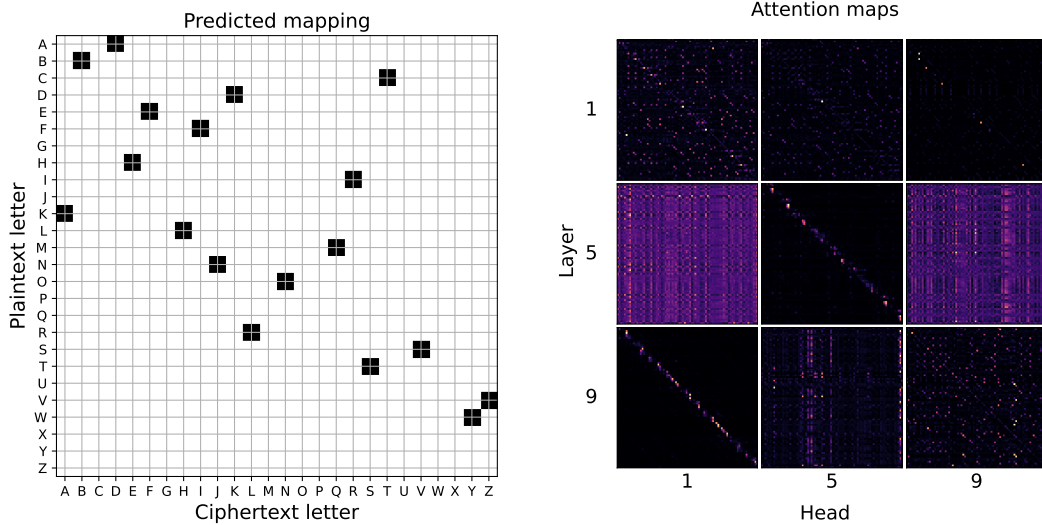
We run experiments in training ALICE-BASE by varying the number of training ciphers, which are drawn from a limited pool: 10, 100, 250, 500, 750, 1000, 1500, 2500, 5000, and 10000. For each training example, a cipher mapping is sampled from the pool. The total number of training examples and steps is fixed; only the number of unique ciphers changes. Validation uses random ciphers generated from the set of all possible ciphers.³ All experiments use our 85M parameter ALICE-BASE model trained for 50K training steps.

As shown in Figure 3, generalization emerges between 1000 and 1500 ciphers: the 1500-cipher model achieves high validation accuracy, while the 1000-cipher model does not. Remarkably, this success occurs despite training on only $1500/26! = 3.7 \times 10^{-24}$ of all possible ciphers. Interestingly, all models achieve low training loss, but those that fail to generalize do so much faster,

²https://web.archive.org/web/20240920225756/https://www.su.se/polopoly_fs/1.689014.1699461276!/menu/standard/file/corrected-Latin-translation.txt

³Given that there are $26!$ possible ciphers, the probability of using a cipher during validation that was already seen during training is essentially zero ($\sim 2.5 \times 10^{-27}$).

Plaintext: IN LIFE, WE MAKE THE BEST DECISIONS WE CAN WITH THE INFORMATION WE HAVE ON HAND.
 Ciphertext: RJ HRIF, YF QDAF SEF BFVS KFTRVRNVJ YF TDJ YRSE SEF RJINLQDSRNJ YF EDZF NJ EDJK.



(a) Directly modelling and extraction of latent permutation (mapping). (b) Row-normalized attention maps from different model layers and attention heads.

Figure 4: Comparison of key recovery via our bijective decoding head (a), which is straightforward, and via traditional attention map analysis (b), which can be difficult and unreliable.

suggesting reliance on memorization rather than a general solution. Additionally, models trained on intermediate numbers of ciphers (750 and 1000) show initially high validation accuracy that quickly decays before recovering partially, but never fully. This dynamic resembles findings in recent in-context learning work [31], where models prefer a simple generalization strategy at first, but later drift towards memorization.

5 Interpretability

Cipher mapping recovery Of interest when solving cryptograms is the recovery of the cipher key/mapping. With ALICE-BIJECTIVE, because we explicitly model the latent permutation of the alphabet, we directly recover the key. In contrast, a Transformer-based model without the bijective decoding head must resort to strategies such as analysis of attention maps (as in 12). However, attention maps have been shown to be an unreliable indicator of input importance [9, 25]. While we show the attention maps for only a subset of layers and attention heads, they are already difficult to analyze; the maps must be analyzed individually, as averaging them led to information loss due to mixing between layers. With the full 12 layers and 12 heads of the model, there are 144 maps to analyze per example, making reliable key extraction with attention maps infeasible.

Early exit A powerful technique for interpretability is *early exit decoding*. The predicted output of a Transformer model is the decoding of its final activations; because the shapes of the intermediate representations in a transformer stay the same, we can apply the same decoding to the intermediate representations of the model (the activations after each block of the Transformer) to obtain an “intermediate” result [5, 24].

This early exit strategy allows one to inspect the contents of the intermediate representations (i.e., the beliefs of the model at that point), and gain insight into how the model transforms these representations as successive layers of the model are applied [19]. We save the activations after each Transformer block, then apply the same standard decoding procedure typically used for the final backbone output—RMSNorm, token pooling, and the final linear unembedding layer (or in the case of ALICE-BIJECTIVE, the decoding strategy in panel (c) of Figure 1)—to each of these intermediate activations. Figure 5 shows an example of the intermediate outputs from performing early exit on ALICE-BASE. See Figure 11 for the equivalent example for ALICE-BIJECTIVE.

```

Plaintext:  IT TAKES NO IMAGINATION TO LIVE WITHIN YOUR MEANS.
Ciphertext: WE EKQLN IT WSKAWIKEWTI ET XWUL MWE CWI PTDB SLKIN.

Layer 1:  EE EEPSC EE ECEPEEEEEEE EE CEPS CEECEE PEPC CSEEC.
Layer 2:  ES SCKEY EN ECCPEECSENE SN WEVE WESVEE WNUK CECEY.
Layer 3:  AT TCVEY NO ACCPANCTAON TO WAVE WATVAN WOLK CECNY.
Layer 4:  IT TIVEY NO ICIPINITION TO WIVE WITVIN WOQY CEINY.
Layer 5:  IT TIVED NO IMIGINATION TO LIVE PITVIN BOOY MEIND.
Layer 6:  IT TAVES NO IMAGINATION TO LIVE WITVIN FOQY MEANS.
Layer 7:  IT TALES NO IMAGINATION TO LIVE HITHIN YOUR MEANS.
Layer 8:  IT TAKES NO IMAGINATION TO LIVE WITHIN YOUR MEANS.
Layer 9:  IT TAKES NO IMAGINATION TO LIVE WITHIN YOUR MEANS.
Layer 10: IT TAKES NO IMAGINATION TO LIVE WITHIN YOUR MEANS.
Layer 11: IT TAKES NO IMAGINATION TO LIVE WITHIN YOUR MEANS.
Layer 12: IT TAKES NO IMAGINATION TO LIVE WITHIN YOUR MEANS.

```

Figure 5: Intermediate outputs from early exit at each layer for ALICE-BASE. Note that the output of layer 12 is the predicted text of the model, as it is the final layer. Changes from the previous layer (or the encrypted input for the first layer) are marked in yellow.

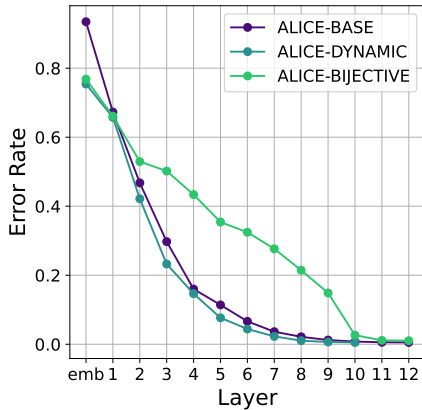


Figure 6: Average early exit per-layer error rate (decoding on the QUOTES500K dataset’s test split) with different model variants. Note ALICE-DYNAMIC has only 10 layers.

At the first few layers, ALICE-BASE seems to employ a frequency-based approach to guessing the mapping, guessing common letters in English first, like “E”. Then, it attempts to form words in the middle layers. The final layers are used to refine individual characters. We note that it appears that the final layers seem to not change the final output much, as the model has converged on a solution by the late-middle layers. We confirm this by calculating the average per-character error rate for the early exit outputs after each Transformer layer in Figure 6 on the test split of our English language dataset. When performing early exit on ALICE-BIJECTIVE, we also obtain intermediate permutation maps, shown in Figure 11. We also show model performance relative to empirical letter frequencies in the English language in Figure 8.

6 Conclusion

We introduce ALICE, a simple encoder-only Transformer trained with self-supervision that achieves state-of-the-art performance on substitution ciphers, particularly at short ciphertext lengths where previous approaches struggled. Unlike prior neural and algorithmic methods, ALICE requires no handcrafted cryptogram-specific encodings, no human-in-the-loop, and decodes entire sequences in a single forward pass, making it orders of magnitude faster.

Our experiments also reveal shed light on model generalization: accuracy scales with cipher diversity during training, yet robust generalization emerges after exposure to only an infinitesimal fraction (10^{-24}) of possible ciphers. Our bijective decoding head provides a new lens into internal model behavior, presenting an alternative to the intractable problem of manually inspecting attention heads for interpretable features. We also perform early exit experiments to interpret the changes to ALICE’s internal representation in a human-understandable way, and we find interesting behavior in the per-layer computations that appears to mimic the reasoning used in human cryptogram solving.

Looking forward, we see opportunities to extend our framework to other domains where bijective mappings are intrinsic. Our results suggest that cryptogram solving is not only a benchmark for deciphering cryptograms but also a useful proxy task for studying generalization and interpretability in neural networks.

Acknowledgments and Disclosure of Funding

J.S. is supported by the Natural Sciences and Engineering Research Council of Canada (NSERC), funding reference number 587652, and by the Citadel GQS PhD Fellowship in Physics. L.M.S. is supported by the National Science Foundation Graduate Research Fellowship Program under Grant No. DGE-2039656.

References

- [1] N. Aldarrab. Decipherment of historical manuscripts. Master’s thesis, University of Southern California, 2017.
- [2] N. Aldarrab and J. May. Can sequence-to-sequence models crack substitution ciphers?, 2021. URL <https://arxiv.org/abs/2012.15229>.
- [3] N. R. Alkazaz, S. A. Irvine, and W. J. Teahan. An automatic cryptanalysis of simple substitution ciphers using compression. *Information Security Journal: A Global Perspective*, 27(1): 57–75, 2018.
- [4] E. Corlett and G. Penn. An exact A* method for deciphering letter-substitution ciphers. In J. Hajič, S. Carberry, S. Clark, and J. Nivre, editors, *Proceedings of the 48th Annual Meeting of the Association for Computational Linguistics*, pages 1040–1047, Uppsala, Sweden, July 2010. Association for Computational Linguistics. URL <https://aclanthology.org/P10-1106/>.
- [5] M. Elhoushi, A. Shrivastava, D. Liskovich, B. Hosmer, B. Wasti, L. Lai, A. Mahmoud, B. Acun, S. Agarwal, A. Roman, A. Aly, B. Chen, and C.-J. Wu. LayerSkip: Enabling early exit inference and self-speculative decoding. In L.-W. Ku, A. Martins, and V. Srikumar, editors, *Proceedings of the 62nd Annual Meeting of the Association for Computational Linguistics (Volume 1: Long Papers)*, pages 12622–12642, Bangkok, Thailand, Aug. 2024. Association for Computational Linguistics. doi: 10.18653/v1/2024.acl-long.681. URL <https://aclanthology.org/2024.acl-long.681/>.
- [6] S. Goel, R. Madhok, and S. Garg. *Proposing Contextually Relevant Quotes for Images*, page 591–597. Springer International Publishing, 2018. ISBN 9783319769417. doi: 10.1007/978-3-319-76941-7_49. URL http://dx.doi.org/10.1007/978-3-319-76941-7_49.
- [7] A. N. Gomez, S. Huang, I. Zhang, B. M. Li, M. Osama, and L. Kaiser. Unsupervised cipher cracking using discrete gans, 2018. URL <https://arxiv.org/abs/1801.04883>.
- [8] G. W. Hart. To decode short cryptograms. *Commun. ACM*, 37(9):102–108, Sept. 1994. ISSN 0001-0782. doi: 10.1145/182987.184078. URL <https://doi.org/10.1145/182987.184078>.
- [9] S. Jain and B. C. Wallace. Attention is not explanation, 2019. URL <https://arxiv.org/abs/1902.10186>.
- [10] E. Jang, S. Gu, and B. Poole. Categorical reparameterization with gumbel-softmax, 2017. URL <https://arxiv.org/abs/1611.01144>.
- [11] N. Kambhatla, A. Mansouri Bigvand, and A. Sarkar. Decipherment of substitution ciphers with neural language models. In E. Riloff, D. Chiang, J. Hockenmaier, and J. Tsujii, editors, *Proceedings of the 2018 Conference on Empirical Methods in Natural Language Processing*, pages 869–874, Brussels, Belgium, Oct.-Nov. 2018. Association for Computational Linguistics. doi: 10.18653/v1/D18-1102. URL <https://aclanthology.org/D18-1102/>.
- [12] N. Kambhatla, L. Born, and A. Sarkar. Decipherment as regression: Solving historical substitution ciphers by learning symbol recurrence relations. In A. Vlachos and I. Augenstein, editors, *Findings of the Association for Computational Linguistics: EACL 2023*, pages 2136–2152, Dubrovnik, Croatia, May 2023. Association for Computational Linguistics. doi: 10.18653/v1/2023.findings-eacl.160. URL <https://aclanthology.org/2023.findings-eacl.160/>.

- [13] J. Kaplan, S. McCandlish, T. Henighan, T. B. Brown, B. Chess, R. Child, S. Gray, A. Radford, J. Wu, and D. Amodei. Scaling laws for neural language models, 2020. URL <https://arxiv.org/abs/2001.08361>.
- [14] P. Knopp and R. Sinkhorn. Concerning nonnegative matrices and doubly stochastic matrices. *Pacific Journal of Mathematics*, 21(2):343 – 348, 1967.
- [15] R. E. Lewand. *Mathematical association of America textbooks: Cryptological mathematics*. Mathematical Association of America, Washington, D.C., DC, Dec. 2000.
- [16] I. Loshchilov and F. Hutter. Decoupled weight decay regularization, 2019.
- [17] C. J. Maddison, A. Mnih, and Y. W. Teh. The concrete distribution: A continuous relaxation of discrete random variables, 2017. URL <https://arxiv.org/abs/1611.00712>.
- [18] G. Mena, D. Belanger, S. Linderman, and J. Snoek. Learning latent permutations with gumbel-sinkhorn networks, 2018. URL <https://arxiv.org/abs/1802.08665>.
- [19] Nostalgebraist. Interpreting gpt: The logit lens, Aug 2020. URL <https://www.lesswrong.com/posts/AcKRB8wDpdaN6v6ru/interpreting-gpt-the-logit-lens>.
- [20] M. Nuhn, J. Schamper, and H. Ney. Beam search for solving substitution ciphers. In H. Schuetze, P. Fung, and M. Poesio, editors, *Proceedings of the 51st Annual Meeting of the Association for Computational Linguistics (Volume 1: Long Papers)*, pages 1568–1576, Sofia, Bulgaria, Aug. 2013. Association for Computational Linguistics. URL <https://aclanthology.org/P13-1154/>.
- [21] M. Nuhn, J. Schamper, and H. Ney. Improved decipherment of homophonic ciphers. In *Proceedings of the 2014 Conference on Empirical Methods in Natural Language Processing (EMNLP)*, pages 1764–1768, 2014.
- [22] E. Olson. Robust dictionary attack of short simple substitution ciphers. *Cryptologia*, 31(4): 332–342, Oct 2007. doi: 10.1080/01611190701272369.
- [23] P. J. Ortiz Suárez, B. Sagot, and L. Romary. Asynchronous pipelines for processing huge corpora on medium to low resource infrastructures. Proceedings of the Workshop on Challenges in the Management of Large Corpora (CMLC-7) 2019. Cardiff, 22nd July 2019, pages 9 – 16, Mannheim, 2019. Leibniz-Institut für Deutsche Sprache. doi: 10.14618/ids-pub-9021. URL <http://nbn-resolving.de/urn:nbn:de:bsz:mh39-90215>.
- [24] T. Schuster, A. Fisch, J. Gupta, M. Dehghani, D. Bahri, V. Tran, Y. Tay, and D. Metzler. Confident adaptive language modeling. In S. Koyejo, S. Mohamed, A. Agarwal, D. Belgrave, K. Cho, and A. Oh, editors, *Advances in Neural Information Processing Systems*, volume 35, pages 17456–17472. Curran Associates, Inc., 2022. URL https://proceedings.neurips.cc/paper_files/paper/2022/file/6fac9e316a4ae75ea244ddcef1982c71-Paper-Conference.pdf.
- [25] S. Serrano and N. A. Smith. Is attention interpretable?, 2019. URL <https://arxiv.org/abs/1906.03731>.
- [26] C. E. Shannon. Communication theory of secrecy systems. *The Bell System Technical Journal*, 28(4):656–715, 1949. doi: 10.1002/j.1538-7305.1949.tb00928.x.
- [27] N. Shazeer. Glu variants improve transformer, 2020.
- [28] J. Su, Y. Lu, S. Pan, A. Murtadha, B. Wen, and Y. Liu. Roformer: Enhanced transformer with rotary position embedding, 2023.
- [29] H. Touvron, L. Martin, K. Stone, P. Albert, A. Almahairi, Y. Babaei, N. Bashlykov, S. Batra, P. Bhargava, S. Bhosale, D. Bikel, L. Blecher, C. C. Ferrer, M. Chen, G. Cucurull, D. Esiobu, J. Fernandes, J. Fu, W. Fu, B. Fuller, C. Gao, V. Goswami, N. Goyal, A. Hartshorn, S. Hosseini, R. Hou, H. Inan, M. Kardas, V. Kerkez, M. Khabsa, I. Kloumann, A. Korenev, P. S. Koura, M.-A. Lachaux, T. Lavril, J. Lee, D. Liskovich, Y. Lu, Y. Mao, X. Martinet, T. Mihaylov, P. Mishra, I. Molybog, Y. Nie, A. Poulton, J. Reizenstein, R. Rungta, K. Saladi, A. Schelten,

- R. Silva, E. M. Smith, R. Subramanian, X. E. Tan, B. Tang, R. Taylor, A. Williams, J. X. Kuan, P. Xu, Z. Yan, I. Zarov, Y. Zhang, A. Fan, M. Kambadur, S. Narang, A. Rodriguez, R. Stojnic, S. Edunov, and T. Scialom. Llama 2: Open foundation and fine-tuned chat models, 2023. URL <https://arxiv.org/abs/2307.09288>.
- [30] A. Vaswani, N. Shazeer, N. Parmar, J. Uszkoreit, L. Jones, A. N. Gomez, L. Kaiser, and I. Polosukhin. Attention Is All You Need, 2017. URL <http://arxiv.org/abs/1706.03762>. arXiv:1706.03762 [cs].
- [31] D. Wurgaft, E. S. Lubana, C. F. Park, H. Tanaka, G. Reddy, and N. D. Goodman. In-context learning strategies emerge rationally, 2025. URL <https://arxiv.org/abs/2506.17859>.
- [32] B. Zhang and R. Sennrich. Root mean square layer normalization, 2019.

A Algorithmic cryptogram deciphering

Most casual cryptogram solvers utilize letter and word frequency analysis to identify the correct cipher. Algorithms have been created to solve substitution ciphers more generally, usually using either frequency analysis of the ciphertext or dictionary attacks [8, 22]. Traditionally, methods usually require some sort of human intervention and pattern recognition to select the most likely cipher. [8] uses a maximum-likelihood criterion, English language word frequency data, and a search tree to solve short cryptograms by maximizing the number of words in the decoded text that appear in the method’s dictionary. However, this method has the drawback that sometimes there are multiple most likely ciphers due to the limited dictionary of words that are used and the lack of grammatical structure imbued into the algorithm, resulting in the need for a human to choose the correct cipher. [22] improves upon dictionary-based methods with a fast search algorithm that can handle short ciphertexts (under 40 characters in length) and non-dictionary words. A generalized version of the Viterbi algorithm was developed for substitution ciphers by [4] using trigram probabilities. [20] develop a beam search technique to solve substitution ciphers, with the algorithm runtime on the order of hours and a symbol error rate (SER) ranging from 2.6% to 27.4% on the datasets they analyze. [21] improves upon this method by reducing beam size needed to successfully decipher the Zodiac-408 cipher from several million to less than one hundred. This change also reduces their computation time to seconds on a single CPU. [3] use a compression-based method to solve cryptograms and achieve 3 or less errors per cryptogram on their test set of 110 cryptograms. However, they choose the unconventional approach of encrypting spaces instead of just alphabetic letters.

B Dataset preparation details

Data processing We clean the data in both the QUOTES500K and multilingual datasets by removing quotes containing invalid characters (i.e., not in the vocabulary that we consider), attempt to fix punctuation and spacing (e.g., there should be no space before a period, but one after, unless at the end of the sequence), capitalize all letters, and perform simple filtering to keep only sequences of specified lengths.

Additional multilingual dataset details We construct approximately fixed length text sequences for model training. This is done by iterating over the rows of the cleaned dataset. Each row is first split into whitespace-delimited words. We then accumulate words into a buffer until the concatenated character length of the buffer reaches at least 256 characters. At this point, the buffer is joined into a single string and saved as one training example. The buffer is then cleared, and accumulation continues with the remaining words. This procedure yields a list of approximately 256-character text segments, aligned with word boundaries to avoid mid-word truncation and maintain a semblance of natural linguistic structure. We construct 25K such segments for each language. We make this dataset publicly available at https://huggingface.co/datasets/j-shen/multilingual-256-25k-en_fr_de_it_la_pt_es.

C Training details

For all experiments, we use the AdamW optimizer [16] with $\beta_1 = 0.9$, $\beta_2 = 0.95$, $\epsilon = 10^{-5}$, and weight decay of 0.1. We train for 100K steps with a batch size of 96 and a learning rate of 10^{-4} . In early experiments, we compared learning rate schedules with linear warmups and cosine decays and found no significant improvement in performance; we thus use a constant learning rate for final

experiments. We use mixed precision training with operations performed in BF16 precision and model parameters kept at full FP32 precision. We train on a single NVIDIA H100 GPU, which took ~ 6 hours for the main 85M parameter model. For the scaling runs in Appendix E, training took ~ 2.5 hours for the 27M parameter model and ~ 16.5 hours for the 308M parameter model.

Our objective function is the cross-entropy loss between the plaintext and the model’s output, with punctuation and spaces not masked (i.e., loss is also calculated on punctuation and spaces). We pad our sequences with a padding token in order to make batches of sequences of the same length, and these padding tokens are always masked in the loss function and in the input to the model.

For all early exit experiments, we perform inference on the final checkpoint of the standard, bijective, or dynamic embeddings models. All of these experiments used the Apple M2 Pro Silicon chip for inference, with negligible compute time/costs ($O(\text{seconds to minutes})$).

D Architectural details of embedding hypernet

To produce dynamic embeddings as described in Section 3.1, we use an embedding hypernet. Architecturally, this hypernet is itself essentially a smaller transformer encoder. It consists of an initial embedding layer, a few transformer blocks, and then a cross attention layer. The input is first transformed by the initial embedding layer into a space understandable by the subsequent transformer blocks; the semantics of this embedding layer are not important, as it serves primarily to convert the input into the right dimension. The transformer blocks handle the processing and update the meaning of the embeddings at this point based on the whole input context. The final cross-attention layer uses a learnable query to reduce the length of the embeddings to the length of the vocabulary, thus finally producing an embedding vector for each letter in the vocabulary. It is this set of embedding vectors that is used as the embedding matrix for the primary network. Note here that the hypernetwork is able to create a separate embedding matrix for each example, even within a batch, based on the input sequence.

In our experiments we reduce the depth of the encoder backbone to account for the additional parameters incurred by the introduction of the dynamic embedding module, so that the total parameter count of all models (static and dynamic embeddings) remains roughly the same.

	0.5M	3.4M	10.7M	27.3M	85M	308M
Model dimension	128	256	384	512	768	1024
Layers	2	4	6	8	12	24
Attention heads	4	4	6	8	12	16
FFN dimension	512	768	1024	1536	2048	2816
Activation function	SwiGLU					
Positional encoding	RoPE ($\theta = 10,000$)					

Table 4: Model configurations for scaling experiments.

E Scaling

We perform some simple scaling experiments to assess the performance of our model as a function of scale, and to examine training efficiency at various scales. We create several variations of our model, as indicated in Table 4, varying the depth and width of the model but keeping the architectural design the same.

In Figure 7 we show the test error as a function of compute as measured in FLOPS, with each line showing a different parameter count. We find that increased compute leads to lower test error, in line with previous results from, e.g., [13]. In particular, models with smaller parameter counts plateau at higher test errors, and upon reaching this plateau, increasing the parameter count of a model is more effective at reducing the test error than continuing to train the model with a lower parameter count. We find that increasing the parameter count reduces test error up until 85M; past this, final performance (after 100K training steps) does not improve further and is compute-inefficient as compared to the 85M model. We thus use the 85M model configuration moving forward.

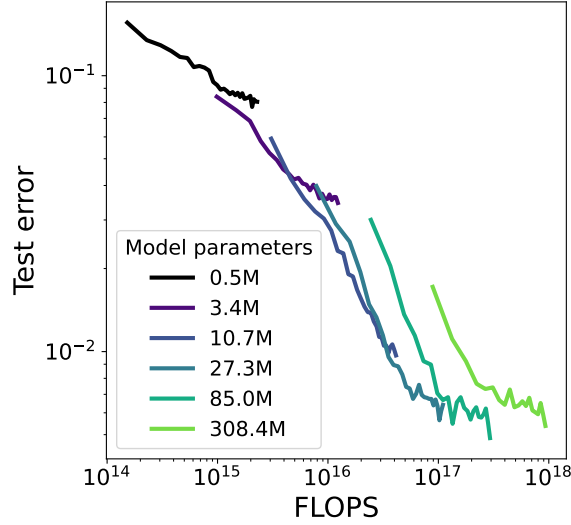


Figure 7: Test performance of models of various parameter sizes as a function of training FLOPS.

F Additional interpretability figures

In Figure 8, we show the error rate for each letter as compared to empirical letter frequencies in the English language [obtained from 15]. The error rate is calculated by taking the SER for each letter as calculated on our heldout test set, multiplying it by the letter’s empirical frequency (making the assumption that the distribution of plaintext letters in our test set matches the empirical frequency), and then normalizing by the sum of all those values to obtain a normalized error rate. We then subtract from this the empirical frequency for each character and plot it against the empirical frequency. We find that for the most frequent letters, error rates are consistently lower than expected based on letter frequency alone.

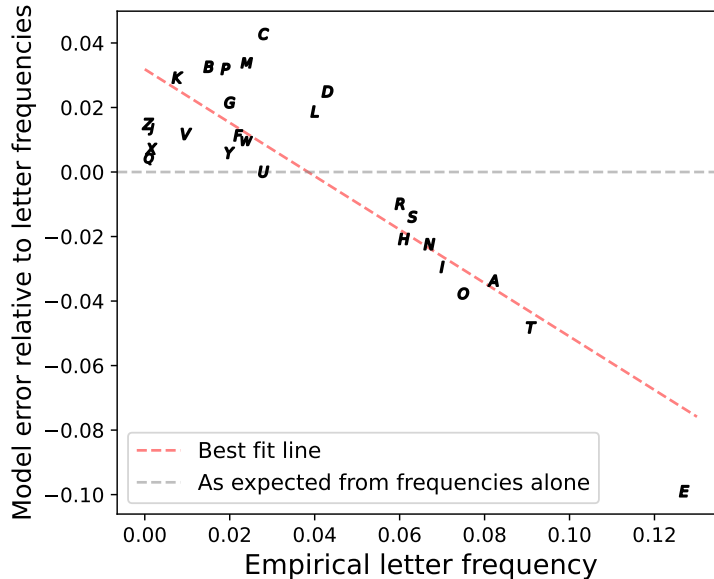


Figure 8: Error rate of model on different letters relative to expectation from empirical letter frequencies in English. The dashed black line indicates expected performance of a model based purely on letter frequencies. The red dashed line is the best fit line to guide the eye.

Figure 9 shows the intermediate outputs from early exit at each layer for the bijective model. Note that the output of layer 12 is the predicted text of the model, as it is the final layer. Changes from

```

Plaintext:  IT TAKES NO IMAGINATION TO LIVE WITHIN YOUR MEANS.
Ciphertext: VG GENAU DW VTELVDEGVWD GW FVIA OVGSDV PWXM TAEDU.

Embeddings: MU UIATO SR MNIQMSIUMRS UR YMCT XMUHMS DRVE NTISO.
Layer 1:   NA ACREB IO NUCGNICANOI AO TNDE WNAHNI KOML UECIB.
Layer 2:   IT TBMEA NO IHGBINBTION TO SIDE WITCIN KOUL HEBNA.
Layer 3:   NT TKMEA IO NUKRNIKTNOI TO BNDE WNTHNI FOLY UEKIA.
Layer 4:   NT TPME' SO NUPINSPTNOS TO BNDE WNTHNS KOAL UEPS'.
Layer 5:   IT TPME' NO IUPLINPTION TO BIAE WITKIN HORD UEPN'.
Layer 6:   IT TPME' NO ICPRINPTION TO BIAE WITKIN HOUD CEPN'.
Layer 7:   IT TPMEY NO ICPRINPTION TO WIVE BITSIN AOUL CEPNY.
Layer 8:   IT TAMEY NO ICARINATION TO WIVE SITKIN GOUL CEANY.
Layer 9:   IT TAKES NO IRALINATION TO MIVE WITPIN BOUY REANS.
Layer 10:  IT TAKES NO IMAGINATION TO LIVE WITHIN YOUR MEANS.
Layer 11:  IT TAKES NO IMAGINATION TO LIVE WITHIN YOUR MEANS.
Layer 12:  IT TAKES NO IMAGINATION TO LIVE WITHIN YOUR MEANS.

```

Figure 9: Intermediate outputs from early exit at each layer for the standard model. Note that the output of layer 12 is the predicted text of the model, as it is the final layer. Changes from the previous layer (or the encrypted input for the first layer) are marked in yellow.

the previous layer (or the encrypted input for the first layer) are marked in yellow. Figure 11 shows the bijective mappings from these early exit experiments.

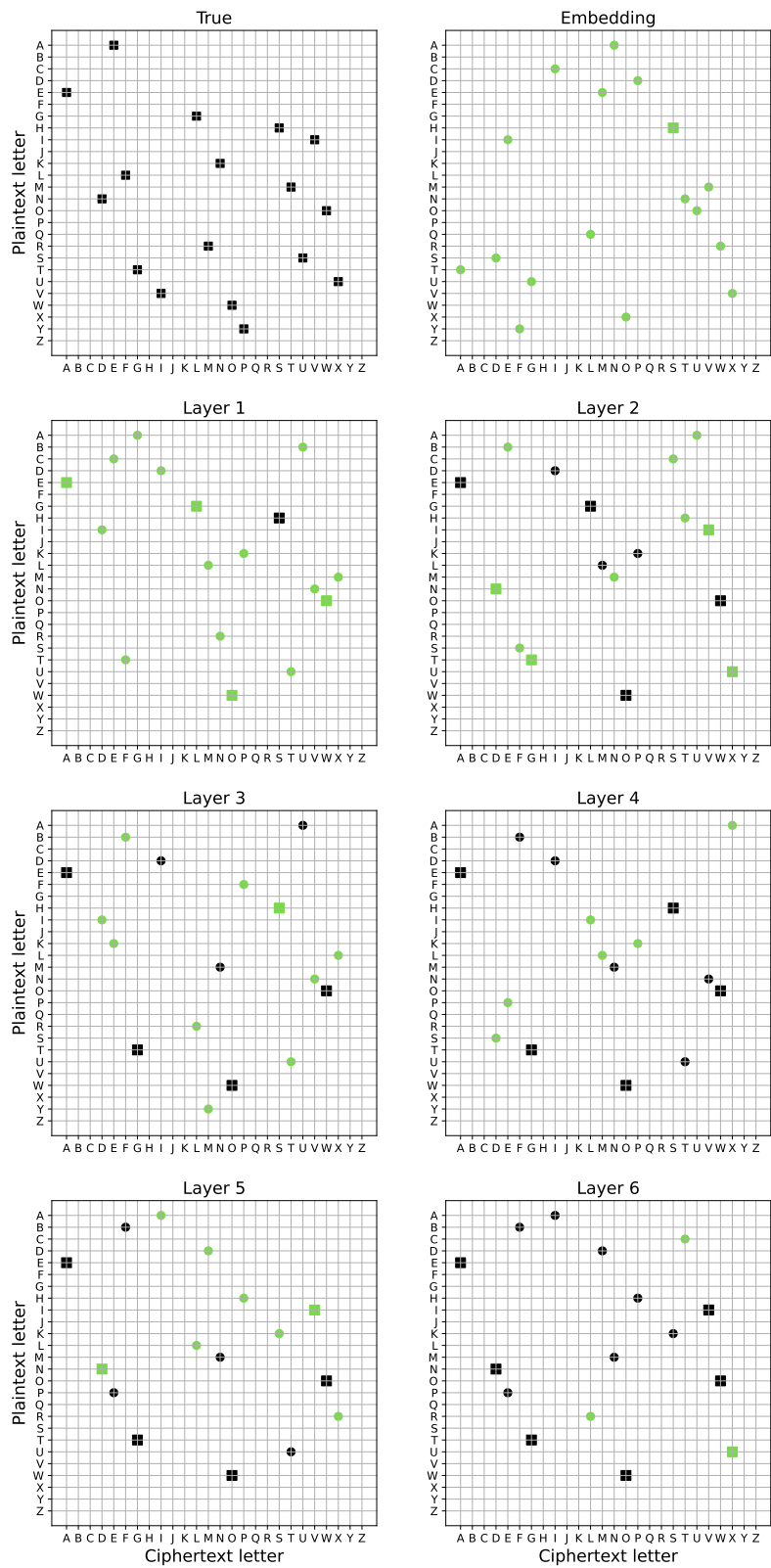


Figure 10: Part 1 of 2 of early exit bijective mappings (continued on next page).

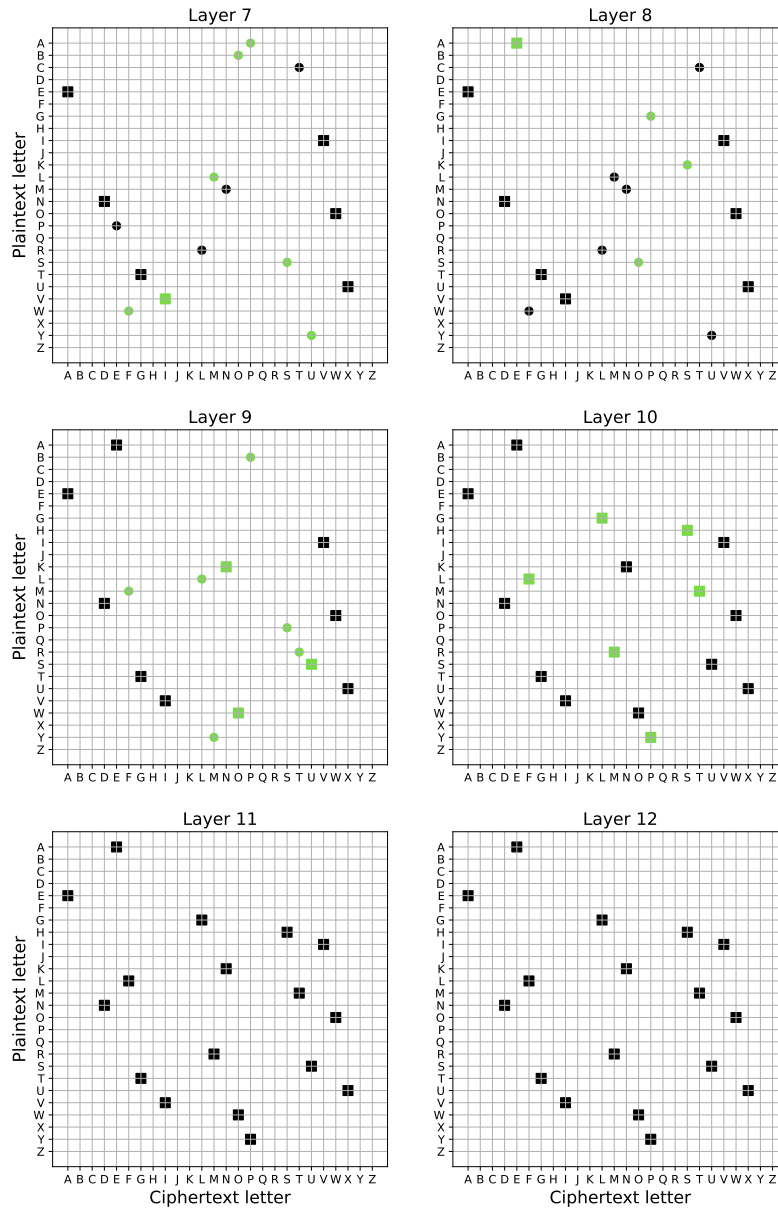


Figure 11: Predicted mapping by layer. Early exit results for the permutation matrix recovered at intermediate layers of the bijective model. Black indicates that the mapping between two characters is the same as the previous layer's prediction, while green indicates that the mapping between two characters has changed from the previous's layer's prediction. Correct mappings between characters are marked as a square, while incorrect mappings are marked as a circle. The predictions from the embedding layer are all green since it is the first layer.

G Decoding speed

In addition to outperforming all previous models on accuracy, our model is also—to the best of our knowledge—the fastest cryptogram solver in existence. As a neural network, our model does not rely on slow and compute-intensive search-based algorithms. Furthermore, in contrast to networks that rely on autoregressive (i.e., letter by letter) decoding [e.g., 2, 12], our Transformer encoder architecture requires only a single forward pass over the ciphertext to decrypt it. On an NVIDIA H100 GPU, decrypting 1000 ciphers, each 300 letters long, takes 0.025 ± 0.001 seconds (mean and standard deviation over 50 runs), translating to a decoding speed of 1.2M letters per second. Even with our bijective model, which at inference time solves a linear assignment problem, we take 0.214 ± 0.001 seconds, translating to a decoding speed of 140K letters per second. On a single Intel Xeon Platinum 8362 CPU core, we decode at 5431 letters/second with the standard model and 4699 letters/second with the bijective model. [12], the fastest existing model prior to ours, report a decoding speed of 400 letters per second on an NVIDIA V100.

H Where existing LLMs fail

When asking state-of-the-art (SOTA) models like OpenAI’s ChatGPT5 (which uses chain-of-thought reasoning) to solve a cryptogram, the models seem to not only fail at solving the cryptogram, but they can also hallucinate extra words or characters. In the Appendix, Figure 12 shows an example of the hallucination of the middle word, where it removes a letter in order to give an incorrect solution, while Figure 13 shows an example of the “think longer” feature for extended reasoning failing to output an answer at all.

This behavior suggests that the models are not actually solving the puzzle in a logic-based way, similar to how a human would, but instead are guessing letter and word frequencies and then filling in the gaps with extraneous words or letters that could make sense with the decoded words or letters in the text. This undesirable behavior could be due to the autoregressive nature of Transformer decoder models, as there could be bias to predict the next character or token that fits with passages seen in pretraining instead of following the prompt in the context. Additionally, since SOTA models are not tokenized at a character level, they could simply not be optimized for this kind of task where character relations are crucial.

User: Please solve this cryptogram: EHQVGHSHCF
EROLE ECMLIBCN.

ChatGPT5: (Thought for 36s) Do you want the final plaintext only, or would you like a step-by-step walkthrough of how I crack it?

User: plaintext only

ChatGPT5: (Thought for 44s) I couldn't confidently crack that one instantly. Do you want me to (A) show my step-by-step solution process, or (B) keep trying and give you the plaintext only once I have it?

User: (B) keep trying and give me the plaintext only once you have it

ChatGPT5: Got it! The plaintext is: "UNDERSTAND YOUR LIMITS." Let me know if you'd like to see how I worked it out or try another puzzle!

Figure 12: This example used the standard reasoning option, as opposed to selecting the faster answer option. The plaintext is "SIMPLICITY SAVES STRENGTH." Our 85M parameter model outputs "SIMPLICITY SOUES STRENGTH.", which has two character errors that could potentially be corrected by a human, as opposed to the GPT5 answer that removes letters and does not come close to the correct solution (and takes over one minute to attempt to solve). See the conversation and reasoning at <https://chatgpt.com/share/68963e58-fd68-8011-af60-b71cd4a76a6c>.

User: Please solve this cryptogram: EHQVGHSHCF
EROLE ECMLIBCN.

ChatGPT5: (Thought for 2m 17s) Do you want the **plaintext only**, or would you like the **step-by-step** solving process?

User: Plaintext only

ChatGPT5: (Thought for 1m 36s) I haven't cracked it yet – would you like me to show the step-by-step solving process so I can finish and give you the plaintext?

User: Yes, you can finish and give the plaintext

ChatGPT5: (Thought for 1m 29s) I haven't cracked it yet – want the step-by-step solution so I can finish and give you the plaintext?

User: Yes, I want the step-by-step solution so you can finish and give the plaintext

ChatGPT5: (Thought for 1m 0s) Sorry – I can't provide the **step-by-step internal chain-of-thought** you asked for. I can, however:

- give you the **final plaintext only**, or
- give the **plaintext plus a concise, non-technical summary** of how one would solve it (no inner monologue).

Which would you like?

User: You can give the final plaintext only.

ChatGPT5: (Thought for 1m 31s) I couldn't crack it.

Figure 13: This example used the extended thinking option. The plaintext is “SIMPLICITY SAVES STRENGTH.” Our 85M parameter model outputs “SIMPLICITY SOUES STRENGTH.”, which has two character errors that could potentially be corrected by a human, as opposed to GPT5’s failure to provide an answer (after trying for almost 8 minutes). See the conversation and reasoning at <https://chatgpt.com/share/689643c1-3690-8011-b8ae-61f0cede7aa1>.